Surface Functionalization of PLGA Nanoparticles for Potential Oral Vaccine Delivery Targeting Intestinal Immune Cells.

Muhammad Khairul Amin and Joshua Boateng.
School of Science, Faculty of Engineering and Science, University of Greenwich, Medway, Kent, ME4 4TB
*Corresponding Author: (J.S.Boateng@gre.ac.uk; joshboat40@gmail.com)

Total number of words = 6579
Total number of tables = 2
Total number of figures = 5

Abstract

This study aimed to develop surface modified PLGA nanocarriers protecting protein-based antigen in the stomach to enable potential release of antigen at target intestinal sites. PLGA nanoparticles (NPs) were prepared by double emulsion and solvent evaporation techniques while surface functionalization was performed using polyethylene glycol (PEG), sodium alginate (ALG) and Eudragit L100 (EUD) with ovalbumin (OVA) as model protein antigen. Nanoparticles were characterized by dynamic light scattering (DLS), scanning electron microscopy (SEM), Fourier-transform infrared spectroscopy (FTIR), gel permeation chromatography (GPC), and stability in simulated gastric fluid (SGF)/simulated intestinal fluid (SIF). Structural integrity of released OVA was analyzed by circular dichroism (CD) and sodium dodecyl sulphate-polyacrylamide gel electrophoresis (SDS-PAGE), while cytotoxicity against Jurkat cells was determined using MTT assay. Surface functionalized PLGA NPs protected the protein in SGF and SIF better than the non-functionalized NPs. Average size of OVA encapsulated NPs was between 235-326 nm and were spherical. FTIR band change was observed after surface modification and showed sustained OVA release compared with the uncoated NPs. The secondary structure of OVA released after 96 hrs remained intact and MTT assay showed >80 % cell viability after 72 hrs while unmodified and surface modified NPs achieved 17 % and 48 % mucin binding respectively. In conclusion, surface modified PLGA NPs have been shown to be safe for potential oral protein-based vaccine delivery.

Keywords: Eudragit, ovalbumin, PLGA nanoparticle, polyethylene glycol, mucosal vaccine, sodium alginate

1. Introduction:

Parenteral administration is the most common way of delivering therapeutic vaccines, however, many biopharmaceuticals are rapidly cleared from the body implying the need for frequent injections (1). Furthermore, parenteral vaccines have high production costs, poor compliance due to fear of needle borne infections, injection site pain and reactogenicity (2). Therefore, there is need for safe and effective alternative delivery systems for protein-based vaccines. The oral route is the most convenient, safe and effective route for drug delivery; however, successful protein delivery is limited by hostile nature of mammalian gastrointestinal tract (GIT) including low gastric pH, poor permeability through the mucosal epithelial barrier, enzymes designed to digest proteins (3). To overcome these challenges, several approaches have been explored for oral vaccine delivery to protect the antigen in the GIT using carriers such as liposomes, nanoparticles and vaccine adjuvants. There are several factors which can influence the effectiveness of administered vaccines, the most critical being the ability to deliver antigens to the target immune induction site and provide high potential for processing by antigen presenting cells (4). In recent decades, it has been reported that polymeric nanoparticles (NPs) can be effectively used for oral antigen delivery. The critical considerations include their toxicity, irritancy, biocompatibility, biodegradability and allergenicity (5).

The synthetic copolymer poly (D, L-lactide-co-glycolide) lactide: glycolide (PLGA) is an aliphatic polyester and one of the most widely used to produce NPs for oral protein delivery (6). Generally, aliphatic polyesters are hydrolytically unstable and easily degrade when in contact with biological fluids and initial degradation of PLGA NPs inside the human body can be as high as 30 % (6). Surface functionalization can significantly increase stability in biological fluids and increase blood circulation half-life of PLGA NPs and duration of action of loaded biomacromolecules (7)(8)(9). NP surface charge also plays a vital role in their interaction with cells and subsequent uptake. Positively charged NPs allow higher extent of internalization and establishing an interaction with negatively charged cell membranes (10) and also able to escape from lysosomes after internalization (11). With this background, the aim of this work was to develop PLGA NPs to potentially deliver therapeutic proteins specially targeted to the intestinal epithelium. For this purpose, three different polymers (sodium alginate, polyethylene glycol and Eudragit) were chosen to chemically modify the surface of PLGA NPs.

The most commonly used hydrophilic moieties are non-ionic polymers such as polyethylene glycol (PEG) (10). PEG is a non-adhesive polymer, but when copolymerized with

PLGA, the PEG shell helps improve the stability of the colloidal system in biological fluids (12). Sodium alginate (ALG) is an anionic and bioadhesive polysaccharide-based polymer used extensively in vaccine and drug delivery research due to its ability to shrink and remain intact at stomach pH and release its cargo at higher intestinal pH (13). The negatively charged PLGA NPs can be changed into a neutral surface charge, thus improving their transport across different mucosa especially intestinal membranes (12)(14). Eudragit (EUD) comprises a diverse range of polymethacrylate- based copolymers. The Eudragit L grade has showed efficacy to protect active ingredients in gastric acid and enhance their therapeutic effectiveness (15), enhance mucoadhesive properties and subsequently uptake of the antigen loaded NPs by the M-Cells in the intestinal Peyer's patches (16).

2. Materials and Methods:

2.1 Materials

PLGA (lactide:glycolide 50:50, MW:30,000-60,000), poly (vinyl alcohol) MW:89000-98000, ovalbumin, 96 % agarose gel, mucin from porcine stomach, glacial acetic acid, calcium chloride, Coomassie brilliant blue, disodium hydrogen phosphate, hydrochloric acid, monobasic potassium dihydrogen phosphate, sodium acetate, sodium azide, sodium bicarbonate, sodium chloride, sodium dihydrogen phosphate, sodium hydroxide, D(+)-trehalose, polyethylene glycol (PEG) (MW-20,000), Bradford protein assay reagent, pepsin from porcine gastric mucosa, sodium taurocholate, lecithin, acetic acid, sodium acetate, maleic acid, sodium oleate, sodium alginate medium viscosity from brown algae, RPMI 1640 medium supplemented with 10 % fetal calf serum, 1 % L-glutamine, 1 % penicillin/streptomycin, fetal bovine serum, MTT (3-(4,5-dimethylthiazol-2-yl)-2,5-diphenyltetrazolium bromide), phosphate buffer (pH 6.8) were purchased from Thermo Fisher Scientific, (Loughborough, UK). 1mM ethylenediamine tetraacetic acid (EDTA), 2-mercaptoethanol and bromophenol blue, sodium dodecyl sulphate-acrylamide gel electrophoresis (SDS-PAGE) were purchased from Bio-Rad, UK. Eudragit L100 was obtained as a gift from Evonik Industries (Germany) and human T lymphocytes (Jurkat cells), 3rd passage were kindly donated by the cell culture laboratory of Dr Giulia Getti (University of Greenwich, Medway, UK).

2.2 Preparation of PLGA NPs

Plain (unmodified) PLGA NPs were prepared by solvent emulsification evaporation and double emulsion (W/O/W) techniques as previously reported (17) with some modifications. Briefly, 100 mg PLGA was dissolved in 5 ml dichloromethane (DCM) and vortexed until a

clear solution was obtained, 0.5 ml PBS (pH 7.4) was added and probe sonicated for 30 s (70 % amplitude) to obtain a primary emulsion. The primary emulsion was added dropwise into 50 ml of 1 % w/v polyvinyl alcohol (PVA) solution, probe sonicated (30 s) and homogenized (12,000 rpm, 5 min) and DCM evaporated with continuous stirring (300 rpm, 6 hrs). The final NP emulsion was centrifuged (Hitachi, CR22G11) (7965 g, 30 min), pellet collected, washed 3x with deionized water, freeze dried and characterized as blank NP.

For OVA encapsulated NPs, formulation process was modified slightly and performed at cold temperature (2-6 ºC) to avoid protein degradation. Different concentrations OVA solutions were added to PLGA DCM solution, probe sonicated (60 s) to obtain the W/O emulsion. The OVA-PLGA mixture was added to 50 ml PVA solution and homogenized (12,000 rpm, 5 min), to form W/O/W emulsion. The emulsion was gently stirred and passed 5x through a 0.8 mm membrane at a nitrogen pressure of 2.0 MPa to obtain OVA loaded PLGA NPs and DCM thoroughly evaporated by stirring (150 rpm, 4 hrs) under ambient conditions. The resulting OVA-PLGA NPs were collected and washed 3x by centrifugation (6452 g). OVA encapsulation was calculated using equation 1:

$$\text{EE}\ (\%) = \frac{\text{Ovalbumin(initial)} - \text{Ovalbumin(supernatent)}}{\text{Ovalbumin (initial)}} \times 100\ \% \ldots . (\text{Eq}..1)$$

2.3 Surface modification of PLGA NPs

PEG and ALG were separately dissolved in deionized water at five different concentrations (0.05 %, 0.1 %, 0.2 %, 0.3 % and 0.4 % w/v). However, EUD L100 was first dissolved in anhydrous methanol Briefly, 0.05, 0.1, 0.2, 0.3 and 0.4 g of EUD L100 was dissolved in 7 ml methanol and vortexed until clear solutions were obtained. Subsequently, the solutions were made up to 100 ml using deionized water to yield final EUD concentrations of 0.05 %, 0.1 %, 0.2 %, 0.3 % and 0.4 % w/v. To obtain the surface modified NPs, freeze dried (100 mg) blank PLGA NPs were dispersed in the different PEG, ALG and EUD solutions and stirred on a magnetic stirrer for 1 hr. The mixture was centrifuged for 30 min (6452 g), and the resultant coated NPs were freeze-dried.

2.4 Analytical characterization

Gel permeation chromatography (GPC) was performed with an Agilent 1100 (Agilent Technologies, Cheshire, UK) system equipped with a refractive index detector. Samples were dissolved (10 mg/ml) in tetrahydrofuran (THF) and injected onto the column (TSK gel G3000PWXL_7.5 mm_30 cm, Tosoh, Tokyo) at a flow rate of 1 ml/min at 30 °C using THF

as mobile phase and pullulan 200,000 as standard. The number average molecular weight (Mn), weight average molecular weight (Mw) and molecular weight dispersity (Dm) were analyzed with Agilent Chem Station software and data plotted with origin pro-2022.

The NPs were evaluated using dynamic light scattering (DLS) by measuring particle size, polydispersity index (PDI) and zeta potential on a Zetasizer Nano-ZS90 (Malvern Instruments, Worcestershire, UK). A disposable cuvette was used for size and PDI analyses while zeta potential was measured using a reusable folded capillary cell, (Malvern Model: DTS1070). Samples were measured in double distilled water, adjusted to a conductivity of 50IS/cm with sodium chloride (0.9 % w/v) with pH range of 5.5-7.5 and 20 V/cm applied field strength. Samples were diluted with dilution medium and scanned (4.65 mm from cuvette wall with an automatic attenuator, 20 °C) with fixed refractive index, viscosity and dielectric constant. Fifteen runs of 10 s were performed, with three replicates (n = 3) for both blank and OVA loaded NPs.

The NPs morphology was examined by SEM (Hitachi SU8030) at operating voltage of 1 kV. One drop of freshly prepared particle suspension was deposited onto sample stub, allowed to air dry and coated with chromium for 3 min. Low voltage (1 kV) was used to observe the NPs to avoid particle deformation and decomposition. FTIR spectra were obtained for pure starting materials and NPs at 20 °C from 4000-450 cm^{-1} at scan rate of 4 cm^{-1}/s using a Perkin Elmer FTIR spectrophotometer. Different peaks in the IR spectrum were interpreted for different functional groups in the formulations.

2.5 NPs stability in biological fluids.

Surface modified NPs were analyzed for stability in simulated gastric fluid (SGF) and simulated intestinal fluid (SIF) using a previously reported method (18). The NPs were dispersed in SGF or SIF contained in round shaped bottles for both blank and protein loaded formulations and placed in a shaking water bath with constant agitation (200 rpm, 37 °C) for 2 and 8 hrs for SGF and SIF respectively. At 30 min intervals, both fluids were sampled, and particles analyzed for size using Zeta sizer and SEM. Further, the withdrawn protein loaded PLGA NPs suspension was passed through Millipore filter and the protein lost from the NPs analyzed.

2.6 *In vitro* protein release study:

OVA release from PLGA NPs was investigated by incubation in SIF (pH 7.4, 37 °C) for 4 days (96 hrs) due to the anticipated slow release because of the surface modification and also

to measure NPs stability in SIF environment. At appropriate time intervals the samples were collected, centrifuged (17133 g, 30 min) and protein concentration in the supernatant determined by Bradford protein assay at 570 nm.

2.7 OVA structural integrity:

Circular dichroism (CD) spectra were obtained using Chirascan spectrophotometer (Applied Photophysics Limited) to examine the secondary structure of OVA after release. Spectra were collected at 20 °C using a quartz cell (180-260 nm, resolution-0.2 nm, 2.25 s response time). Noise reduction, blank solution subtraction and data analyses were performed using standard temperature/wavelength analysis program (Origin pro-8, USA)). OVA was extracted from samples after 96 hrs of *in vitro* release study by centrifuging at 885 g before CD analysis and compared with native OVA. Each spectrum represents an average of four consecutive scans.

Sodium dodecyl sulfate-polyacrylamide gel electrophoresis (SDS-PAGE) analysis was performed on OVA released from the PLGA NPs after 96 hrs in SIF (pH 6.8). Aliquots (20 ml) of the dispersions were mixed with similar volume of SDS loading buffer and heated (80 °C, 10 min) to denature the proteins, cooled to room temperature and centrifuged to remove any suspended solids. Aliquots (15 μl) of the supernatant were transferred to the polyacrylamide gradient gel and electrophoresis performed (180 V, 120 min) (19). Tris-HCl, pH 6.8, 1mM EDTA and bromophenol blue served as tracking agents with 2-mercaptoethanol as reducing agent. The gel was stained with Coomassie blue staining solution and washed with 5 % (v/v) acetic acid solution overnight. Images were captured by UV-visible imaging system (Geldoc).

2.8 Cell culture:

Jurkat cells (2×10^5 cells/ml) were cultured in RPMI 1640 medium supplemented with 10 % FBS and 1 % (v/v) of L-glutamine, penicillin and streptomycin. The cells were cultivated in an incubator (37 °C, 5 % CO_2, 95 % relative humidity) (Heracell 150i CO incubator, Thermo Scientific) according to company protocol. Briefly, 1 ml aliquot of cells was thawed quickly in water bath (37 °C) and transferred to 9 ml warm media in a 15 ml conical tube, mixed gently and centrifuged (51 g, 5 min). The media was discarded, pellet gently re-suspended in 10 ml warm medium, and cells divided into two T-25 flasks containing 5 ml warm media and placed in the incubator. After 48 hrs, the media was removed and replaced with fresh media.

2.10 *In vitro* cell viability:

Cell viability (MTT) assay was used to evaluate the toxicity of the NPs according to manufacturer instructions (ATCC, USA). Aliquots (300 µl) of the Jurkat cell suspension prepared above was added to each well of 8-well plates and incubated (37 °C, 4 hrs). Cells were treated for 24, 48 and 72 hrs after seeding in 96-well plates with 20, 60, 100, 200 and 500 µg/ml of NPs using untreated cells used as control. Interfering NPs were removed by centrifugation at 1200 rpm and absorbance was measured at 540 nm using a Multiscan plate reader.

2.11 *In vitro* mucin binding:

Mucoadhesive properties of PLGA NPs were investigated as previously described (20). Briefly, mucin solution (0.5 ml, 0.5 mg/ml) was mixed with 0.5 ml of surface modified NP suspension incubated in a shaking water bath (37 °C, 2 hrs). The suspension was centrifuged (9062 g, 40 min), supernatant collected and free mucin analyzed using Bradford assay. The supernatant was incubated with Bradford reagent for 5 min in a 96 well plate, and absorbance (620 nm) measured with auto absorbance reader (Multiskan FC Microplate Photometer, Thermo Fisher Scientific). Mucin concentration was calculated from a standard curve of mucin (0.1-1.0 mg/ml) and amount of mucin binding with NPs was measured by equation (1).

2.12 Statistical analysis

Statistical analysis was carried out for all the quantitative data using Microsoft Excel 2021 and GraphPad prism (version 9, USA). Results were analyzed by one way ANOVA followed by Tukey's HSD test (0.05) for DLS data. When the *p*-values <0.05, differences were considered statistically significant.

3. Results and discussion:

3.1 Dynamic light scattering:

Different concentrations of coating materials (Figure S1 & S2) were used to modify the surface of the PLGA NPs to obtain optimum formulations based on size distribution, PDI and zeta potential values. Both plain and coated NPs showed nanometer size distribution and expected to accumulate at the target intestinal site by passive mechanisms, enhance permeation and prolonged systemic circulation (21). Uncoated blank NPs showed, particle size of 221±8 nm, PDI of 0.21±0.3 and zeta potential of +17±4 mV. The amount of surfactant plays an important role during emulsification and the solvent evaporation process by protecting the PLGA droplets (NPs) against coalescence (22). Table 1 showed that the NPs size increased significantly ($p <$

0.05) after PEG modification (255±4 nm) and further increased to 298±23 nm after OVA encapsulation.

Table 1: DLS results (particle size, PDI and zeta potential) for selected optimum NPs (n = 3). Details in Figures S1 and S2.

Formulation	Particle size (nm ± SD)		Zeta potential (mV ± SD)		PDI (± SD)	
	Blank	OVA loaded	Blank	OVA loaded	Blank	OVA loaded
PLGA-Uncoated	221 ± 8	235 ± 21	+17 ± 4	-22 ± 4	0.21 ± 0.03	0.24 ± 0.07
PLGA-PEG	255 ± 4	298 ± 23	-17 ± 4	-27 ± 6	0.32 ± 0.03	0.32 ± 0.09
PLGA-ALG	276 ± 4	301 ± 12	-18 ± 2	-24 ± 9	0.43 ± 0.04	0.38 ± 0.08
PLGA-EUD	312 ± 17	326 ± 14	-20 ± 4	-24 ± 4	0.31 ± 0.02	0.45 ± 0.04

This could be because the low starting concentration of PLGA (0.1 % w/v) was suppressed by the higher concentration (1.0 % w/v) of PVA. This might be because the anionic PEG was oriented outside the NPs and exposed at its terminal end. Further, surface charge is an important factor affecting aggregation of NPs and therefore colloidal stability. Blank PLGA-PEG NPs showed zeta potential value of -17 ± 4 mV while the OVA loaded equivalent was -27 ± 6 mV at PEG concentration of 0.1 %. PEG has negative to neutral charge and non-covalently binds and anchors on PLGA NPs surface forming a negative surface charge (23) which prevents interarticular aggregation by stearic repulsion. Interestingly, increasing the concentration (Figure S1 & S2 of PEG (0.2 % to 0.5 %) caused a significant ($p < 0.05$) decrease in the zeta potential resulting in agglomeration and precipitation and consequent significant increase in size and PDI. Based on these observations the NPs obtained from PLGA: PEG (1:1) was determined as optimum.

The size and PDI for ALG coated NPs increased significantly ($p < 0.05$) to 276 ± 4 nm and 0.43 ± 0.8 respectively which was consistent with previously published work (24). Upon dispersion in water, ALG produces larger swollen chains polymer which may be localized on the outer surface of the initial PLGA NPs droplets causing increased intrinsic viscosity leading to larger particles (25). OVA loaded PLGA-ALG NPs increased in size with increasing ALG concentration (Figure S1 & S2) while the protein loading efficiency decreased with increasing initial OVA concentration (Figure S3). The former observation is probably due to high viscosity of the ALG in the external phase which produces larger emulsion droplets and ultimately larger particles. This also correlates with SEM images (Figure S4) with average size

of 150-800 nm. Zeta potential significantly decreased from -24 ± 9 mV to -11.8 ± 2 mV for 0.1 and 0.5 % ALG respectively, because at higher ALG concentrations more polyelectrolytes might associate with the NPs surface, decreasing zeta potential and causing aggregation(26). Based on the above results, NPs obtained from 1:1 ratio of PLGA: ALG was determined as optimum formulation for further study.

Compared with blank PEG (0.1 %) and ALG (0.1 %) modification, optimum EUD modified PLGA NPs was determined at 0.05 % with size and zeta potential of 312 ± 17 nm and -20 ± 4 mV respectively. At 0.1–0.05 % EUD, NP size significantly increased due to factors such as pH of the organic solvent and presence of methacrylic acid esters (27). However, methacrylic acid on the PLGA NPs surface is expected to improve mucoadhesion to enhance transport across intestinal membrane. Zeta potential decreased significantly from -24.63 ± 4 to -4.4 ± 1 mV at EUD concentration of 0.05 and 0.5 % respectively (Figure S4).

3.2 SEM analysis

Representative SEM micrographs are shown in Figure 1 (A, C) with . spherical shapes and no aggregation. Mean particle size ranged between 100–500 nm, while particle size distribution histograms (Figure 1-B, D) showed range between 100-400 nm, both in agreement with DLS data. The optimized coated PLGA-PEG-Blank and PLGA-PEG-OVA NPs exhibited a globular morphology with the formation spherical shape (Figure S1). Figure S4(a) showed uncoated PLGA NPs were concentrated in colloidal emulsion with heterogenous size distribution resulting in particles aggregation.

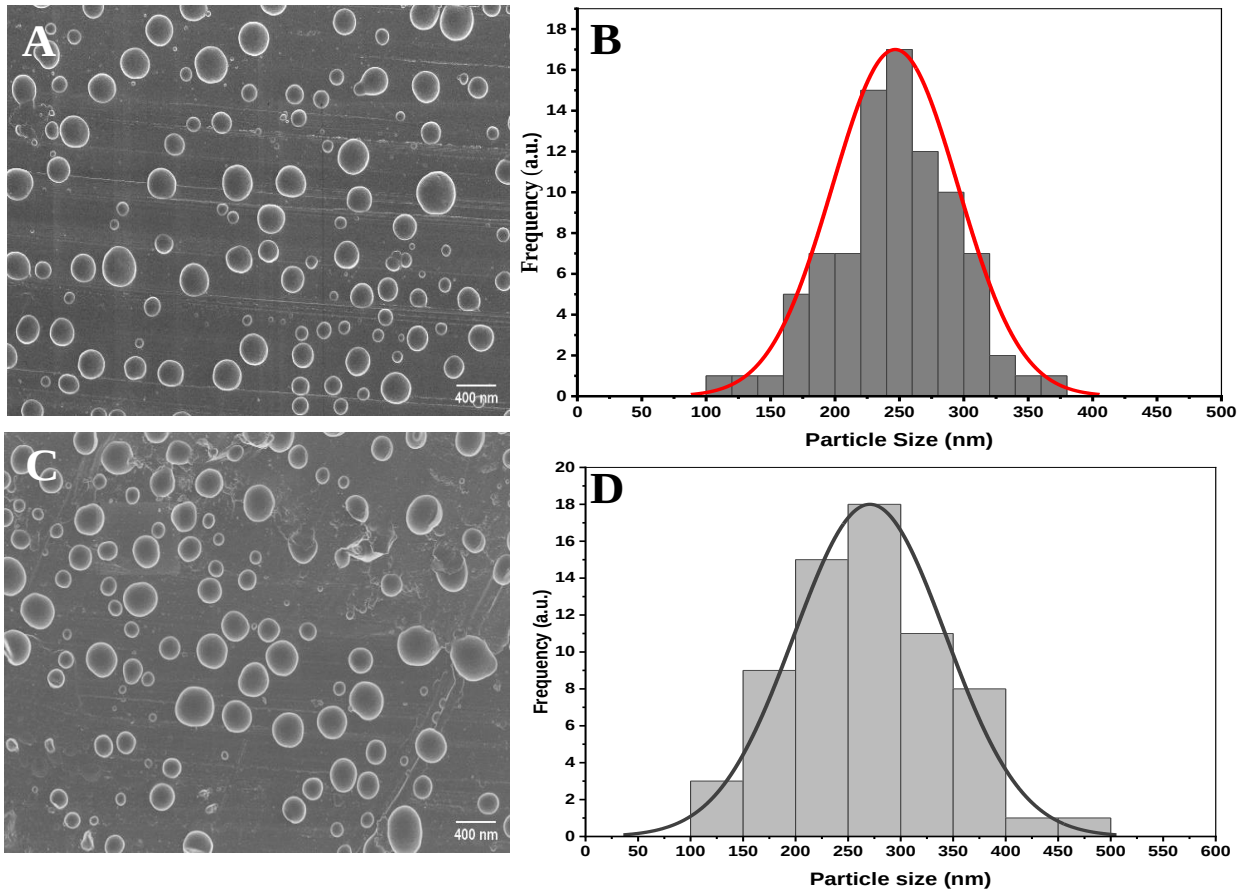

Figure 1 SEM images of blank (A and C) and OVA loaded (B and D) PLGA-PEG NPs showing corresponding particle dimension analysis by image j software.

After surface functionalization with ALG (Figure S4b) slightly better homogeneous distribution was observed though PDI was still high (0.43 ± 0.04). The EUD coated NPs showed lower little cluster formation, however, the presence of hydrogen bonds in the aqueous dispersion phase of the emulsion leads to some flocculation as evident from Figure S4(c). In Figure S4(d-f) it was confirmed that coating affects particles size and OVA might be binding on the outer surface of PLGA NPs.

3.3 FTIR analysis

Pure PLGA, showed medium intense bands in the region of 1700-1800 cm^{-1} (Figure S5) attributed to stretching vibration of carbonyl groups in lactide and glycolide and same bands was observed in Figure 2 and S6 at 1790-1800 cm^{-1} for the NPs. Bands at 1100 cm^{-1} were attributed to asymmetric and symmetric C-C-O stretches, characteristic of esters. The common peaks at 2800-3100 cm^{-1} are stretching vibration regions of -OH, -CH (alkene), -CH

(alkane) and -NH functional groups (Figure 2 a-d). Physical interaction between the amino group of OVA and keto group of PLGA might take place in the region 2800-3100 cm^{-1} by formation of weak bonds such as van der Waal forces dipole moment or weak hydrogen bond (28). Stretching vibration between 900-600 cm^{-1} represent C-CL, C-Br and C-C functional groups (Figure 2, a-d). Bands at 3350 cm^{-1} were attributed to unreacted carboxyl groups from PLGA. OVA loaded PLGA-PEG NPs showed a broad band around 3500 cm^{-1} related to the O-H groups. The peaks at 3240 cm^{-1} from PEG coated PLGA NPs in Figure 2 confirm the NH stretch while 900 cm^{-1} shows N-H bending with the peak at 1680 cm^{-1} corresponding to C=O stretch. EUD coated PLGA NPs showed peaks at 1654 cm^{-1} attributed to C=O stretching, 1382 cm^{-1} corresponding to $-CH_3$ stretching, 2120 $cm^{-1}$and 2130 cm^{-1} indicates NH_2 of PLGA-EUD-OVA formulation.

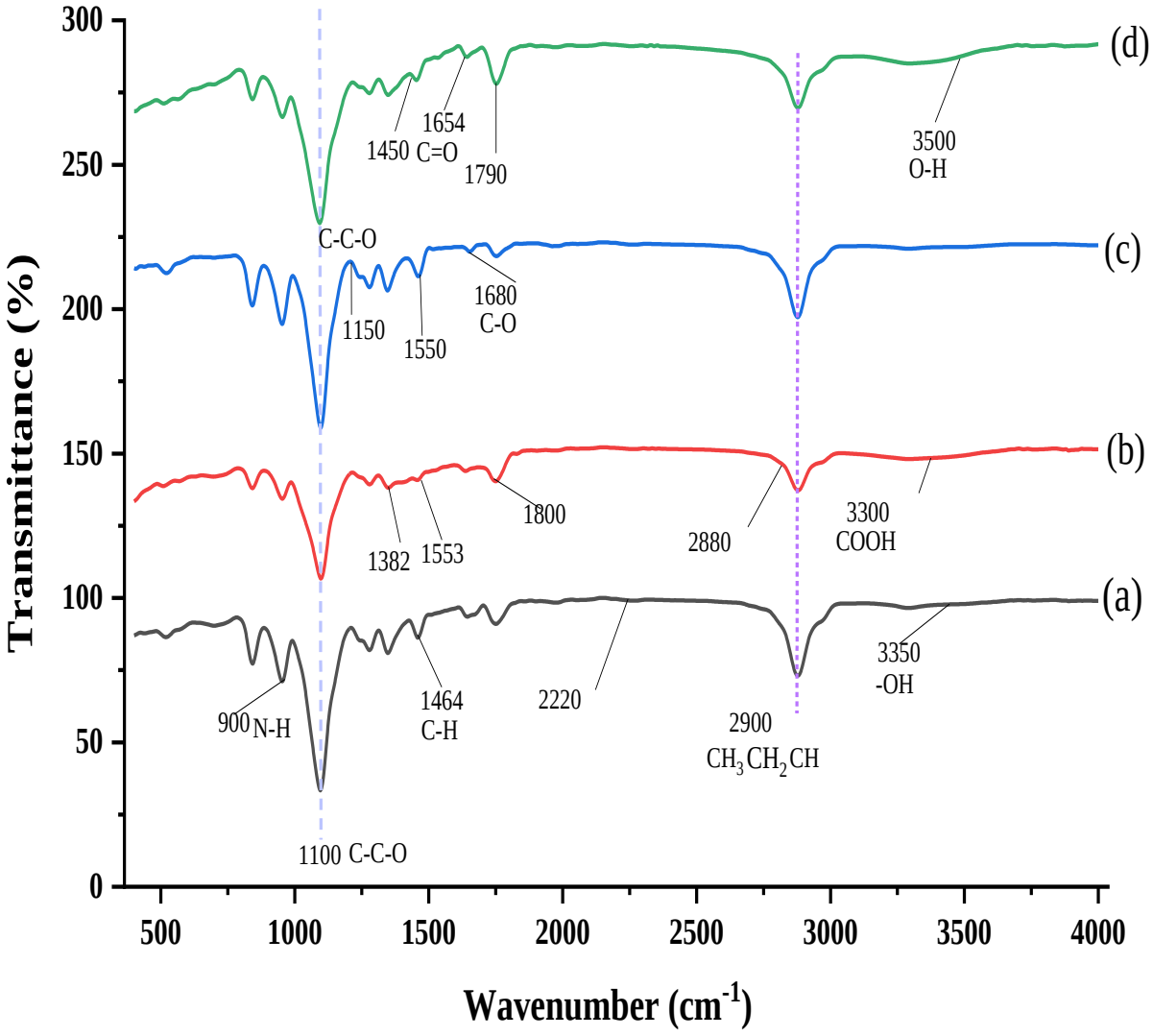

Figure 2 FTIR spectra of OVA loaded NPs (a) PLGA-OVA (b) PLGA-PEG-OVA (C) PLGA-ALG-OVA (d) PLGA-EUD-OVA.

3.4 GPC analysis:

PLGA can be degraded by the emulsification process and any MW change can be measured by GPC. Table S1 summarizes the GPC results for the starting materials and NPs. The GPC pattern shows the depolymerization and chain scission process when MW of pure materials and NPs are compared (Figure 3 (A,B). During NPs formulation, PLGA can undergo several end terminal modifications such as ester end capping of it is free COOH end group which is an important factor that affecting it's the hydrophilicity with ester being more hydrophobic than COOH end groups (29).

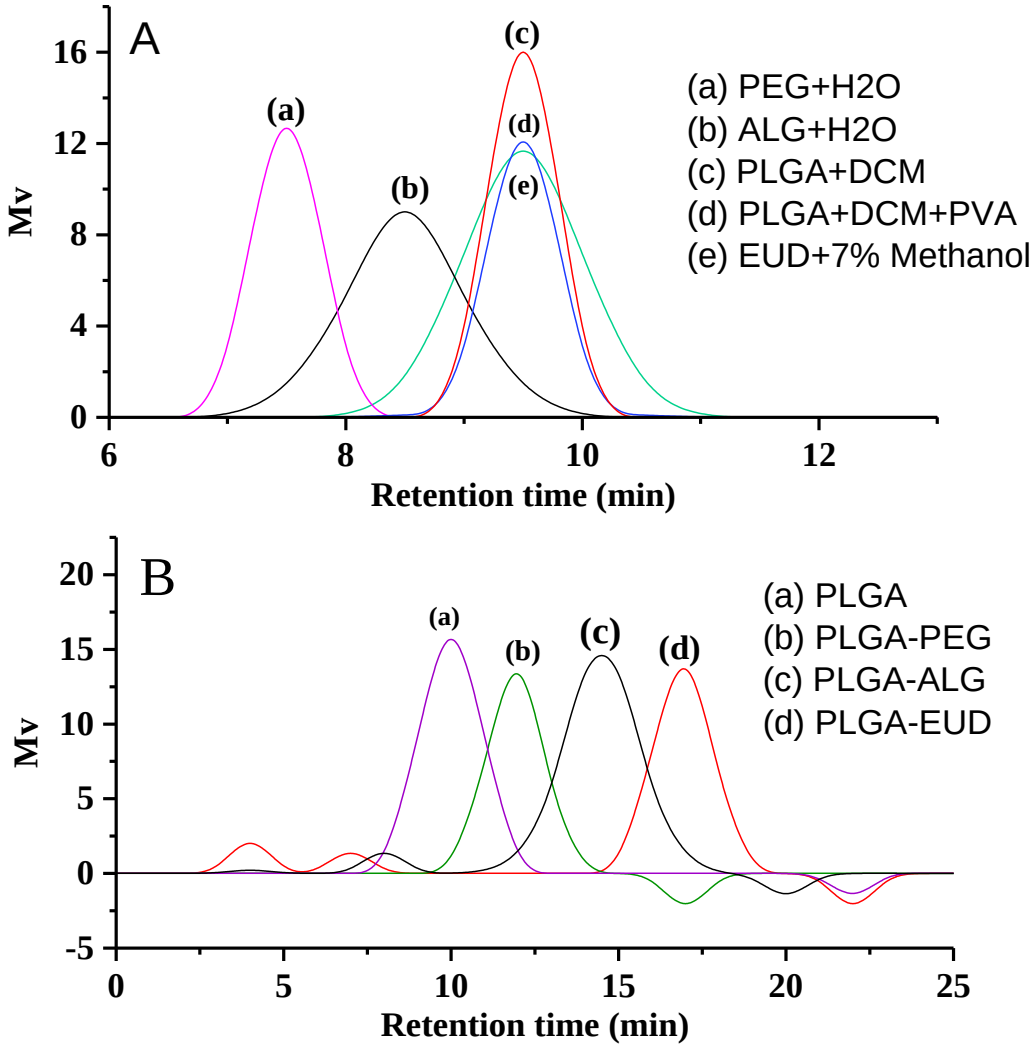

Figure 3: Gel permeation chromatography analysis for molecular weight distribution of (A) pure starting materials and (B) NP formulations.

Calculation of weight average molecular weight (Mw), number average molecular weight (Mn) and molecular weight dispersity (Dm) was achieved with equations i to iii (Table S1, Figure S7) as reported (30). The GPC results showed that the Mn and Mw of starting materials shifted to longer retention times in the formulations. The Dm of the pure materials and NPs was in the range of 1.12-1.55 which fits well with the theoretical value. The GPC profile of the filtered mixed PLGA-PEG sample showed no significant change of Mw, with the starting PLGA having Mw of 37300 Da while PLGA-PEG showed about 33015 Da (Table S1). This suggests that any deleterious effects of the formulation process was prevented by the presence of long PLGA polymer chains. Interestingly, more PLGA was retained on the formulation, because the NPs indicates peaks eluting between 7-9 min, mirroring starting PLGA peaks observed between 6-9 min (Figure 3B). GPC profile of the PLGA-PEG NPs exhibited no bimodal peaks which could be due to the favorable mixing of PLGA and PEG. However, PLGA-ALG peaks showed bimodal peaks at retention time of 13-16 min (main) and small monomodal peaks at 5-7 min corresponding to the pure ALG. This might be due to degradation of ALG or polymer scission induced by the formulation process. At the concentrations used, multimolecular aggregates are not believed to be formed, instead smaller monomolecular units (unimers) exist where the molecules undergo a conformational change and it is hypothesized that hydrophobic chain segment is coiled in its interior and shielded by the ALG units (31).

3.5 Stability of NPs in biological fluids

To develop a successful protein carrier to target intestinal sites, particle stability is important to protect encapsulated protein from the harsh gastrointestinal environment. The colloidal stability of PLGA NPs in SGF and SIF was investigated by monitoring particle size (Figure 4). The diameter of uncoated PLGA NPs was 235 nm initially but decreased to 170 nm after 70 min and significantly ($p < 0.05$) decreased to 80 nm within 2 hrs. This could be attributed to pepsin breaking the ester bond from the PLGA backbone and acidic pH (1.2) causing erosion of the particle surface via hydrolysis (32)(33). The size of PLGA-ALG-OVA remained relatively stable in SGF with no significant reduction over 120 min with the initial particle size of 295 nm decreasing to only 210 nm after 2 hrs. This slight reduction could be attributed to enzymatic degradation although particle diameter is determined by the balance between the

polymer viscosity and interfacial tension (34). Figure 4A shows that PEG also confers stability to PLGA NPs in SGF for at least 2 hrs but with some size reduction. The presence PEG chains on NPs surface provides a hydrophilic layer which influences the reduced particle size observed generally, due to a spontaneous deionization of free carboxyl end groups on the particle (35). Due to its methacrylic acid functional groups, EUD has pH dependent solubility and its swelling and erosion occurred at pH of 1.2, hence the significant size reduction.

However, unlike the ALG and PEG coated formulations, the PLGA-EUD-OVA NPs showed significant ($p < 0.05$) size reduction after 60 min and indicating particle instability in SGF.

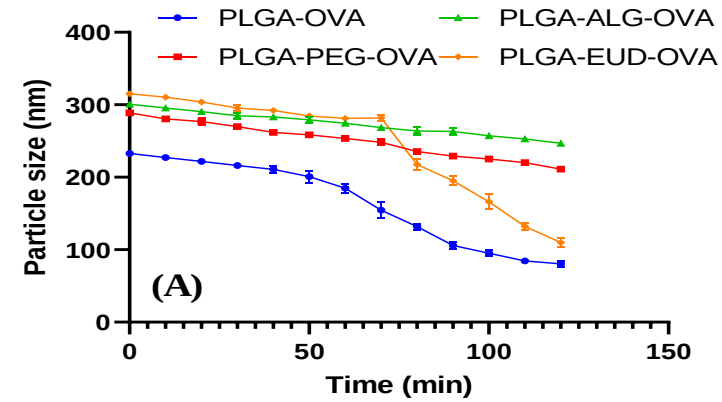

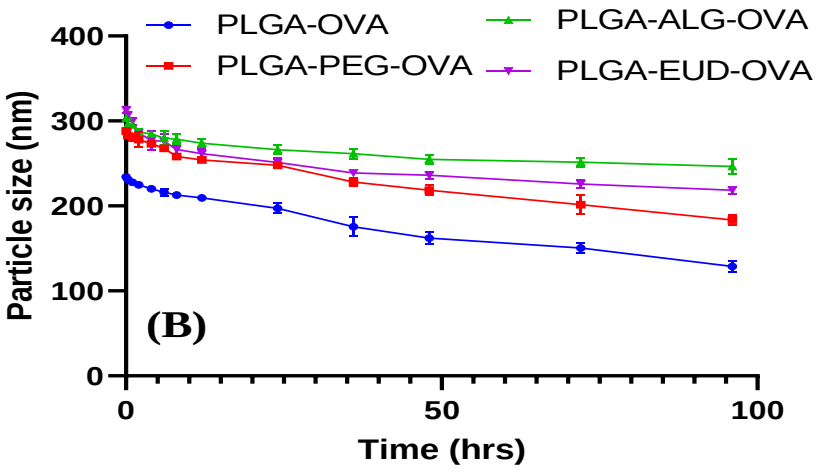

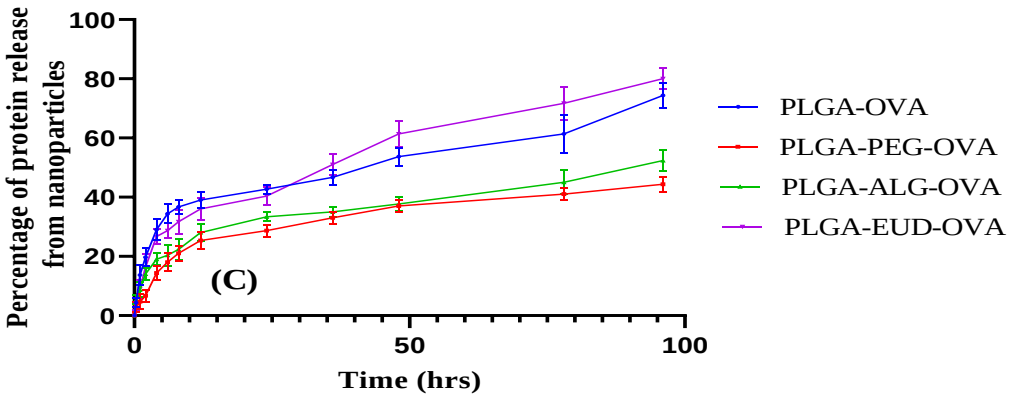

Figure 4 Stability profiles of PLGA NPs in (A) SGF, (B) SIF based on size measurements and (C) *in vitro* protein release in SIF.

The size of the modified OVA loaded NPs in SIF showed longer term stability over 96 hrs, compared to SGF (Figure 4B). Generally, uncoated PLGA NPs showed a sharp, significant reduction in particle size from 235 nm to 128 nm, however, the sizes of the PEG, ALG and EUD coated NPs reduced more gradually and not significant. Once again, the PLGA-ALG formulation showed the most stable particle size over 96 hrs because the pKa of mannuronic and guluronic acid residues of ALG are 3.38 and 3.65 respectively. Therefore, at lower pH (SGF), the pKa of the uronic acids are stabilized by intermolecular hydrogen bonding networks (34) and particles are only slowly degraded upon contact with SIF. Interestingly, the EUD coated PLGA NPs remained stable in SIF which could be due to being dissolved in 7 % methanol which potentially increases hydrophobicity of the outer surface leading to slower swelling and erosion in SIF.

3.6 *In vitro* OVA release

Significant burst effect was observed for uncoated NPs, with 30 % protein released over 6 hrs (Figure 4C) but coated NPs showed only 5-15 % OVA released in 6 hrs. The lowest burst release was for PLGA-ALG NPs where the electrostatic attraction between PLGA and ALG could slow protein release. The initial burst release from coated NPs, could be attributed to small amounts of protein bound on their outer surface and more readily displaced by dissolution medium.

The initial burst effect was followed by a more sustained release after 10 hrs. The cumulative release of OVA within 96 hrs was 78 % from uncoated NPs whereas, ALG and PEG coated NPs achieved 53 % and 48 % release respectively, which could be due to smaller uncoated NPs possessing higher surface area. Further, PLGA-PEG NPs having smaller sizes also exhibited faster release than the larger PLGA-ALG NPs. Interestingly, PLGA-EUD NPs showed higher cumulative release similar to the uncoated NPs, suggesting that protein release does not only depend on particle size but also on other factors such as porosity, layer thickness and density, chain conformation, electrostatic interaction or repulsion which influence protein diffusion through the layer. Overall, it is probable that after OVA was released from PEG and ALG coated NPs, it was subsequently bound to the outer shell which caused further delay in their release. The binding might be due to the interaction between OVA and a few hydrophobic amino acids and hydrophobic segments involved in OVA shell (36). Exposure of PLGA NPs to basic conditions can induce structural transformations in OVA, including increasing its

hydrophobicity and enhance its propensity to produce insoluble aggregates that can ultimately impact OVA release (37).

3.7 OVA structural integrity:

Potential conformational changes in OVA were analyzed by SDS-PAGE and Figure 5A, showed no additional bands that would indicate the presence of covalent aggregates or fragments and was comparable with standard monomeric OVA. The band near 43 kDa suggest that NPs formulation and protein loading parameters does not affect the protein structure, implying the native structure of OVA was maintained after release from PLGA NPs.

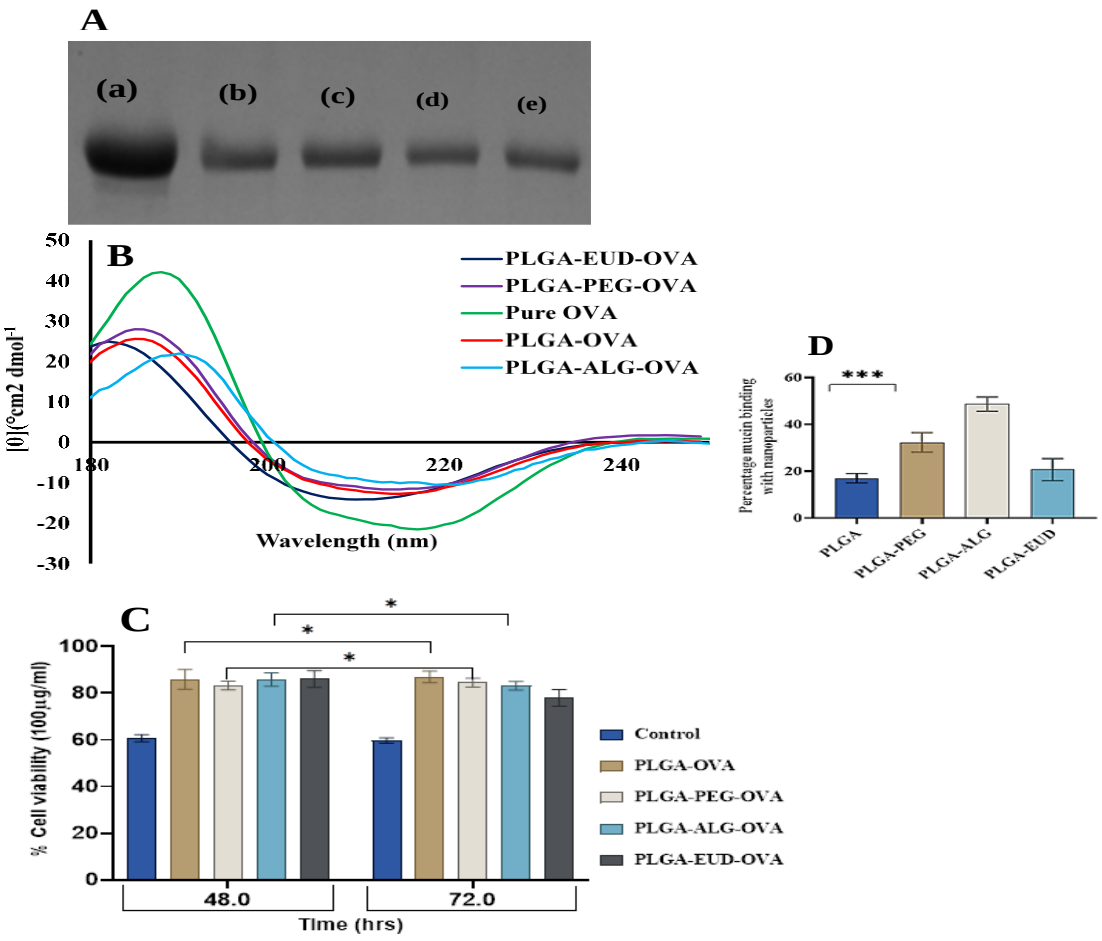

Figure 5: (**A**) SDS-PAGE profiles of OVA released from NPs: (a) pure OVA (b) OVA released from uncoated PLGA NPs; (c) OVA released from PLGA-ALG NPs (d) OVA released from PLGA-PEG NPs; (e) OVA released from PLGA-EUD NPs (all after 48 hrs). (**B**) CD spectra of OVA released from PLGA NPs after 96 hrs. (**C**) *In vitro* call viability results of PLGA NPs in contact with Jurkat cells after 48 hrs and 72 hrs. (**D**) mucin binding results of PLGA NPs.

Further, OVA secondary structure was evaluated with CD (Figure 5B) after 96 hrs of OVA release from the NPs in the presence of SIF (38,39) The average ratios of α-helix and β-sheet and random coils in intact samples were 32 %, 46 % and 22 % respectively (Table 2) indicating

that the percentage α-helical and β-sheet occupied 78 % of the secondary structure for native OVA. Uncoated and OVA loaded PLGA NPs showed ratios of 29 % α-helix, 44 %-β sheet and 27 %, random coil respectively which was relatively similar to native OVA.

Table 2: CD data of OVA showing relative percentages for α-helices, β sheets and random coils.

OVA	α-helix (%)	β-sheet (%)	Random coil (%)
Pure OVA	32 ± 2	46 ± 3	22 ± 0
PLGA-OVA	29 ± 1	44 ± 2	27 ± 3
PLGA-PEG-OVA	26 ± 2	39 ± 1	35 ± 3
PLGA-ALG-OVA	28 ± 2	41 ± 2	31 ± 2
PLGA-EUD-OVA	25 ± 3	42 ± 3	33 ± 3

The differences in shape and intensity of peaks between native OVA and OVA released from NPs (Figure 5B) were very small with only a slight loss of α-helix for protein released, indicating that the helicity of OVA was preserved. It is known(38) that protein exposure to solvents can affect its structure, therefore DCM used to dissolve PLGA could have caused the small change in α-helicity. The CD spectra of pure OVA compared with that released from NPs showed slight change at 205nm peak corresponding to β-sheet domains, which might be due to hydrophobic interactions between protein molecule and PLGA NPs (FTIR results) and previously reported (40)(41) This further confirms that secondary structure of OVA was not perturbed by the complexation, organic solvent, homogenization, sonication and SIF.

3.8 *In vitro* cell viability:

Cell viability assay was performed to confirm their biocompatibility and potential use for vaccine delivery. According to Figure S8 (A,B) all the blank and NPs containing OVA concentration between 20-100 µg/ml were non-toxic with cell viability around 85 %. Further, no toxic effects were observed up to 72 hrs (Figure 5C) for the optimized PLGA-ALG-OVA and PLGA-PEG-OVA formulations, however, the PLGA-EUD-OVA NPs showed considerably lower cell viability (74 %) at OVA concentration of 100 µg/ml. This may be due to NPs size dependent toxicity that increased the reactivity of these NPs with the cell (42). The PLGA-EUD-OVA NPs showed larger size (326 nm) and higher PDI (0.45±0.4) (table 1)

compared with the other formulations, which may cause instability in the cell culture medium, leading to higher cell disruption.

3.9 *In vitro* mucin binding

Mucin binding with NP surface is an important criterion for mucoadhesive formulation development. Figure 5D shows mucin binding results of coated and uncoated blank PLGA NPs. PLGA-PEG NPs showed 33 % mucin binding while PLGA-EUD NPs showed 21 % mucin binding. This may have occurred because of lower concentration of EUD (0.05 %) employed in the optimized PLGA-EUD NPs. PLGA-ALG formulation showed highest (48 %) mucin binding because ALG has abundant hydroxyl and ether groups, which interact with mucin and increase the bond forming groups, enhancing the mucoadhesive performance (43). Finally, uncoated PLGA NPs with positive charge (Table 1) only achieved 17 % mucin binding, contrary to previously reported studies (44) and confirms that the NPs surface properties is not the only criterion determining mucoadhesive behavior of NPs. In general, mucin can bind with polymeric NPs surface through covalent or noncovalent interactions that forms a size exclusion barrier to molecules, particles or pathogens (45).

4. Conclusion:

Optimized PLGA NPs were formulated using different coating agents. Particle size increased after coating and OVA loading with low PDI and high zeta potential indicating uniform size distribution and good stability respectively. PLGA-PEG and PLGA-ALG NPs were more stable than the uncoated NPs and PLGA-EUD NPs in SGF (2 hrs) and SIF (96 hrs). CD and SDS-PAGE analysis showed that secondary structures of the released OVA were maintained while optimized PLGA NPs showed >80 % cell viability after 72 hrs. The ALG coated NPs showed highest mucin binding and sustained release of protein and seem to be optimum formulation for potential protein-based antigen delivery to trigger mucosal immune response. However, further in vivo studies are required to confirm these.

Authors contributions: **Muhammad Amin**: Methodology, Visualization, Investigation Data curation, Writing – original draft. **Joshua Boateng**: Conceptualization, Supervision, Resources, Investigation, Visualization, Review and re-writing of original draft.

References:

1. S. Mitragotri, P.A. Burke, R. Langer, Overcoming the challenges in administering biopharmaceuticals: Formulation and delivery strategies. Nature Reviews Drug Discovery, 2014,13(9),655–672.
2. S. Mitragotri, Immunization without needles. Nature Reviews Immunology, 2005, 5(12), 905–916.
3. S.H. Bakhru, S. Furtado, A.P. Morello, E. Mathiowitz, Oral delivery of proteins by biodegradable nanoparticles. Advanced Drug Delivery Reviews, 2013, 65(6), 811-821.
4. M.R. Neutra, P.A. Kozlowski, Mucosal vaccines, The promise and the challenge. Nature Reviews Immunology, 2006, 6, 148–158.
5. T. Akagi, M. Akashi, Development of polymeric nanoparticles-based vaccine. Nihon Rinsho, 2006, 64(2), 279-285.
6. R.A. Jain, The manufacturing techniques of various drug loaded biodegradable poly(lactide-co-glycolide) (PLGA) devices. Biomaterials, 2000, 21(23), 2475-2490.
7. S. Derman, Z.A. Mustafaeva, E.S. Abamor, M. Bagirova, A. Allahverdiyev, Preparation, characterization and immunological evaluation: canine parvovirus synthetic peptide loaded PLGA nanoparticles. J Biomed Sci, 2015, 22(89), 1-12.
8. F. Danhier, E. Ansorena, J.M. Silva, R. Coco, A.L. Breton, V. Préat, PLGA-based nanoparticles: An overview of biomedical applications. Journal of Controlled Release, 2012, 161(2):505-522.
9. D. Blanco and M.J. Alonso, Protein encapsulation and release from poly(lactide-co-glycolide) microspheres: Effect of the protein and polymer properties and of the co-encapsulation of surfactants. European Journal of Pharmaceutics and Biopharmaceutics, 1998, 45(3), 285-294.
10. Y.R. Lee, Y.H. Lee, S.A. Im, K. Kim, C.K. Lee, Formulation and Characterization of Antigen-loaded PLGA Nanoparticles for Efficient Cross-priming of the Antigen. Immune Network, 2011, 11(3), 163–168.
11. P.N. Gupta, K. Khatri, A.K. Goyal, N. Mishra, Vyas SP. M-cell targeted biodegradable PLGA nanoparticles for oral immunization against hepatitis B. Journal of Drug Targeting, 2007, 15(10),701-713.
12. Y. Cu, W.M. Saltzman, Controlled surface modification with poly(ethylene)glycol enhances diffusion of PLGA nanoparticles in human cervical Mucus. Molecular Pharmaceutics, 2009, 6(1), 173–181.
13. X.Y. Li, X.Y. Kong, S. Shi, X.L. Zheng, G. Guo, Y.Q. Wei, Z.Y. Qian, Preparation of alginate coated chitosan microparticles for vaccine delivery. BMC Biotechnology, 2008, 8(89), 1-11.
14. D.N. Kapoor, A. Bhatia, R. Kaur, R. Sharma, G. Kaur, S. Dhawan, PLGA: A unique polymer for drug delivery. Therapeutic Delivery, 2015, 6(1), 41-58.
15. D. Kapoor, R. Maheshwari, K. Verma, S. Sharma, P. Ghode, R.K. Tekade, Coating technologies in pharmaceutical product development. In: Drug Delivery Systems, 2019, Chapter 14, 665–719.
16. M. Cetin, A. Atila, Y. Kadioglu, Formulation and in vitro characterization of Eudragit® L100 and Eudragit® L100-PLGA nanoparticles containing diclofenac sodium. AAPS PharmSciTech, 2010, 11(3), 1250–1266.
17. M.K. Amin, J.S. Boateng, Comparison and process optimization of PLGA, chitosan and silica nanoparticles for potential oral vaccine delivery. Therapeutic Delivery. 2019, 10(8), 493-514.

18. G. Mittal, H. Carswell, R. Brett, S. Currie, M.N.V.R. Kumar, Development and evaluation of polymer nanoparticles for oral delivery of estradiol to rat brain in a model of Alzheimer's pathology. Journal of Controlled Release, 2011, 150(2), 220–228.
19. B. Liu, Y. Pang, R. Bouhenni, E. Duah, S. Paruchuri, L. McDonald L, A step toward simplified detection of serum albumin on SDS-PAGE using an environment-sensitive flavone sensor. Chemical Communications, 2015, 51, 11060-11063.
20. S. Dyawanapelly, U. Koli, V. Dharamdasani, R. Jain, P. Dandekar, Improved mucoadhesion and cell uptake of chitosan and chitosan oligosaccharide surface-modified polymer nanoparticles for mucosal delivery of proteins. Drug Delivery and Translational Research, 2016, 6(4), 365–379.
21. Y.S. Nam, J.Y. Park, S.H. Han, I.S. Chang, Intracellular drug delivery using poly(D,L-lactide-co-glycolide) nanoparticles derivatized with a peptide from a transcriptional activator protein of HIV-1. Biotechnology Letters, 2002, 24, 2093–2098.
22. K.Y. Hernández-Giottonini, R.J. Rodríguez-Córdova, C.A. Gutiérrez-Valenzuela, O. Peñuñuri-Miranda, P. Zavala-Rivera, P. Guerrero-Germán, A.L. Acuña, PLGA nanoparticle preparations by emulsification and nanoprecipitation techniques: Effects of formulation parameters. RSC Advances. Royal Society of Chemistry, 2020, 10, 4218–4231.
23. S.H. Kim, J.H. Jeong, K.W. Chun, T.G. Park, Target-specific cellular uptake of PLGA nanoparticles coated with poly(L-lysine)-poly(ethylene glycol)-folate conjugate. Langmuir, 2005, 21(19), 8852–8857.
24. S. Abdelghany, T. Parumasivam, A. Pang, B. Roediger, P. Tang, K. Jahn, H.K. Chan, Alginate modified-PLGA nanoparticles entrapping amikacin and moxifloxacin as a novel host-directed therapy for multidrug-resistant tuberculosis. Journal of Drug Delivery Science and Technology, 2019, 1(52), 642–651.
25. J. Nesamony, P.R. Singh, S.E. Nada, Z.A. Shah, W.M. Kolling, Calcium alginate nanoparticles synthesized through a novel interfacial cross-linking method as a potential protein drug delivery system. Journal of Pharmaceutical Sciences, 2012, 101(6), 2177–2184.
26. Q. Wang, S. Jamal, M.S. Detamore, C. Berkland, PLGA-chitosan/PLGA-alginate nanoparticle blends as biodegradable colloidal gels for seeding human umbilical cord mesenchymal stem cells. Journal of Biomedical Materials Research, 2011, 1(96), 520–527.
27. F. Bahman, K. Greish, S. Taurin, Insulin nanoformulations for nonparenteral administration in diabetic patients. Theory and Applications of Nonparenteral Nanomedicines, 2021, 409–43.
28. V. Sainz, C. Peres, T. Ciman, C. Rodrigues, A.S. Viana, C.A.M. Afonso, Optimization of protein loaded PLGA nanoparticle manufacturing parameters following a quality-by-design approach. RSC Advances, 2016, 6(106), 104502–104512.
29. K.Y. Hernández-Giottonini , R.J. Rodríguez-Córdova, C.A. Gutiérrez-Valenzuela, O. Peñuñuri-Miranda, P. Zavala-Rivera, P. Guerrero-Germán, A.L. Acuña, PLGA nanoparticle preparations by emulsification and nanoprecipitation techniques: Effects of formulation parameters. RSC Advances. Royal Society of Chemistry, 2020, 10, 4218–4231.
30. L. Chen, T. Ci, T. Li, L. Yu, J. Ding, Effects of molecular weight distribution of amphiphilic block copolymers on their solubility, micellization, and temperature-induced sol-gel transition in water. Macromolecules, 2014, 47(17):5895–5903.
31. S.A. Hagan, A.G.A. Coombes, M.C. Garnett, S.E. Dunn, M.C. Davies, L. Illum, S. S. Davis, S. E. Harding, S. Purkiss, and P. R. Gellert, Polylactide-Poly(ethylene glycol) Copolymers as

Drug Delivery Systems. Characterization of Water Dispersible Micelle-Forming Systems, 1996, 12(9), 2153–2161.
32. H.K. Makadia, S.J. Siegel, Poly Lactic-co-Glycolic Acid (PLGA) as biodegradable controlled drug delivery carrier. Polymers (Basel), 2011, 3(3), 1377-1397.
33. M.J. Santander-Ortega, D. Bastos-González, J.L. Ortega-Vinuesa, M.J. Alonso, Insulin-loaded PLGA nanoparticles for oral administration: An in vitro physico-chemical characterization. Journal of Biomedical Nanotechnology, 2009, 5(1), 45–53.
34. J.J. Chuang, Y.Y. Huang, S.H. Lo, T.F. Hsu, W.Y. Huang, S.L. Huang, et al. Effects of pH on the Shape of Alginate Particles and Its Release Behavior. International Journal of Polymer Science. 2017, 2017, 1-9.
35. M. Colombo, L. Morelli, S. Gimondi, M. Sevieri, L. Salvioni, M. Guizzetti, B. Colzani, L. Palugan, A. Foppoli, L. Talamini, L. Morosi, M. Zucchetti, M. B. Violatto, L. Russo, M. Salmona, D. Prosperi, M. Colombo, P. Bigini, Monitoring the fate of orally administered PLGA nanoformulation for local delivery of therapeutic drugs. Pharmaceutics, 2019, 11(12).
36. V. Sainz, C. Peres, T. Ciman, C. Rodrigues, A.S. Viana, C.A.M. Afonso, Optimization of protein loaded PLGA nanoparticle manufacturing parameters following a quality-by-design approach. RSC Advances, 2016, 6(106), 104502–104512.
37. A. Wusiman, P. Gu, Z. Liu, S. Xu, Y. Zhang, Y. Hu, J. Liu, D. Wang, X. Huang, Cationic polymer modified PLGA nanoparticles encapsulating alhagi honey polysaccharides as a vaccine delivery system for ovalbumin to improve immune responses. International Journal of Nanomedicine, 2019, 14, 3221–3234.
38. J.H. Espinoza, E. Reynaga-Hernández, J. Ruiz-García, G. Montero-Morán, M. Sanchez-Dominguez, Mercado-Uribe H. Effects of green and red light in βl-crystallin and ovalbumin. Scientific Reports, 2015, 14(5), 1-7.
39. L. Sheng, G. Tang, Q. Wang, J. Zou, M. Ma, X. Huang, Molecular characteristics and foaming properties of ovalbumin-pullulan conjugates through the Maillard reaction. Food Hydrocolloids, 2020, 1(100), 1-7.
40. J. Park, P.M. Fong, J. Lu, K.S. Russell, C.J. Booth, W.M. Saltzman, PEGylated PLGA nanoparticles for the improved delivery of doxorubicin. Nanomedicine: Nanotechnology, Biology, and Medicine., 2009, 5(4), 410–418.
41. B. Mukherjee, K. Santra, G. Pattnaik, S. Ghosh, Preparation, characterization and in-vitro evaluation of sustained release protein-loaded nanoparticles based on biodegradable polymers. International Journal of Nanomedicine, 2008, 3(4), 487–496.
42. L.G. dos Reis, W.H. Lee, M. Svolos, L.M. Moir, R. Jaber, N. Windhab, P.M. Young, D. Traini, Nanotoxicologic effects of PLGA nanoparticles formulated with a cell-penetrating peptide: Searching for a safe pDNA delivery system for the lungs. Pharmaceutics, 2019, 11(1),
43. K. Kesavan, G. Nath, J.K. Pandit, Sodium alginate based mucoadhesive system for gatifloxacin and its in vitro antibacterial activity. Scientia Pharmaceutica, 2010, 78(4), 941–57.
44. S. Bonengel, M. Jelkmann, S. Oh, A. Mahmood, M. Ijaz, A.B. Schnürch, Charge changing phosphorylated polymers: Proof of in situ mucoadhesive properties. European Journal of Pharmaceutics and Biopharmaceutics, 2016, 105, 203–208.
45. G. Petrou, T. Crouzier, Mucins as multifunctional building blocks of biomaterials. Biomaterials Science. Royal Society of Chemistry, 2018, 6, 2282–2297.